172 *Inorg. Chem.* **2011**, *50*, 172–177
DOI: 10.1021/ic1015498

Inorganic Chemistry
Article

Impact of Metal-Ion Dependence on the Porous and Electronic Properties of TCNQ-Dianion-Based Porous Coordination Polymers

Satoru Shimomura,[†] Nobuhiro Yanai,[†] Ryotaro Matsuda,[‡] and Susumu Kitagawa*[,†,‡,§]

[†]*Department of Synthetic Chemistry and Biological Chemistry, Graduate School of Engineering, Kyoto University, Katsura, Kyoto 615−8510, Japan,* [‡]*ERATO Kitagawa Integrated Pores Project (Japan), Kyoto Research Park Bldg #3, Shimogyo-ku, Kyoto 600-8815, Japan, and* [§]*Institute for Integrated Cell-Material Sciences, Kyoto University 69 Konoe-cho, Yoshida, Sakyo-ku, Kyoto 606-8501, Japan*

Received August 2, 2010

A series of TCNQ-dianion-based porous coordination polymers [M(TCNQ)bpy] (M = Fe, Zn, Mn, Co, Cd) have been synthesized and characterized. The synthesis reactions of these compounds are promoted by the addition of ascorbic acid, which is the key to obtaining a high yield. They form almost identical three-dimensional pillared layer structures with the M−TCNQ two-dimensional layers linked by bpy pillar ligands. The electronic properties of these compounds vary depending on the constitutional metal ions and guest molecules. We found that the electronic interaction between metal ions and TCNQ moieties in the frameworks strongly impacted the electronic properties of the compounds.

Introduction

Soft porous crystals (SPCs) with the cooperative integration of "softness" and "regularity" are attractive materials showing unconventional porous properties and unique host−guest interactions.[1] Within the field of SPCs, porous coordination polymers (PCPs) have attracted much attention from scientists because of their remarkably rich diversity of structures and properties.[2−11] In addition, there have been many studies on PCPs having switchable properties that depend on guest molecules, and they have had important ramifications in materials science.[12−28]

PCPs possess an enormous diversity of structures and properties. In many cases, the diversity derives from the infinite variation of organic ligands. The molecular shapes of the organic ligands, which form the pore walls, directly affect the size, shape, and dimensionality of the pore. In addition, their electronic natures and physical properties critically influence the pore surface properties. In contrast,

*To whom correspondence should be addressed. Phone: +81-75-383-2733. Fax: +81-75-383-2732. E-mail: kitagawa@icems.kyoto-u.ac.jp.

(1) Horike, S.; Shimomura, S.; Kitagawa, S. *Nat. Chem.* **2009**, *1*, 695–704.
(2) Eddaoudi, M.; Moler, D. B.; Li, H. L.; Chen, B. L.; Reineke, T. M.; O'Keeffe, M.; Yaghi, O. M. *Acc. Chem. Res.* **2001**, *34*, 319–330.
(3) Kitagawa, S.; Kitaura, R.; Noro, S. *Angew. Chem., Int. Ed.* **2004**, *43*, 2334–2375.
(4) Fletcher, A. J.; Thomas, K. M.; Rosseinsky, M. J. *J. Solid State Chem.* **2005**, *178*, 2491–2510.
(5) Lin, X.; Jia, J. H.; Hubberstey, P.; Schroder, M.; Champness, N. R. *CrystEngComm* **2007**, *9*, 438–448.
(6) Kuppler, R. J.; Timmons, D. J.; Fang, Q. R.; Li, J. R.; Makal, T. A.; Young, M. D.; Yuan, D. Q.; Zhao, D.; Zhuang, W. J.; Zhou, H. C. *Coord. Chem. Rev.* **2009**, *253*, 3042–3066.
(7) Long, J. R.; Yaghi, O. M. *Chem. Soc. Rev.* **2009**, *38*, 1213–1214.
(8) Fischer, R. A.; Woll, C. *Angew. Chem., Int. Ed.* **2009**, *48*, 6205–6208.
(9) Ma, L. Q.; Abney, C.; Lin, W. B. *Chem. Soc. Rev.* **2009**, *38*, 1248–1256.
(10) Ferey, G.; Serre, C. *Chem. Soc. Rev.* **2009**, *38*, 1380–1399.
(11) Deng, H. X.; Olson, M. A.; Stoddart, J. F.; Yaghi, O. M. *Nat. Chem.* **2010**, *2*, 439–443.
(12) Beauvais, L. G.; Shores, M. P.; Long, J. R. *J. Am. Chem. Soc.* **2000**, *122*, 2763–2772.
(13) Ohmori, O.; Kawano, M.; Fujita, M. *J. Am. Chem. Soc.* **2004**, *126*, 16292–16293.
(14) Yao, Q. X.; Pan, L.; Jin, X. H.; Li, J.; Ju, Z. F.; Zhang, J. *Chem.—Eur. J.* **2009**, *15*, 11890–11897.
(15) Yang, S. H.; Lin, X.; Blake, A. J.; Walker, G. S.; Hubberstey, P.; Champness, N. R.; Schroder, M. *Nat. Chem.* **2009**, *1*, 487–493.
(16) Mulfort, K. L.; Wilson, T. M.; Wasielewski, M. R.; Hupp, J. T. *Langmuir* **2009**, *25*, 503–508.
(17) Lee, E. Y.; Jang, S. Y.; Suh, M. P. *J. Am. Chem. Soc.* **2005**, *127*, 6374–6381.
(18) Tanaka, D.; Horike, S.; Kitagawa, S.; Ohba, M.; Hasegawa, M.; Ozawa, Y.; Toriumi, K. *Chem. Commun.* **2007**, 3142–3144.
(19) Hou, L.; Lin, Y. Y.; Chen, X. M. *Inorg. Chem.* **2008**, *47*, 1346–1351.
(20) Chen, B. L.; Wang, L. B.; Xiao, Y. Q.; Fronczek, F. R.; Xue, M.; Cui, Y. J.; Qian, G. D. *Angew. Chem., Int. Ed.* **2009**, *48*, 500–503.
(21) Allendorf, M. D.; Bauer, C. A.; Bhakta, R. K.; Houk, R. J. T. *Chem. Soc. Rev.* **2009**, *38*, 1330–1352.
(22) Muller, M.; Devaux, A.; Yang, C. H.; De Cola, L.; Fischer, R. A. *Photochem. Photobiol. Sci* **2010**, *9*, 846–853.
(23) Fuma, Y.; Ebihara, M.; Kutsumizu, S.; Kawamura, T. *J. Am. Chem. Soc.* **2004**, *126*, 12238–12239.
(24) Zeng, M. H.; Wang, Q. X.; Tan, Y. X.; Hu, S.; Zhao, H. X.; Long, L. S.; Kurmoo, M. *J. Am. Chem. Soc.* **2010**, *132*, 2561–2563.
(25) Maspoch, D.; Ruiz-Molina, D.; Wurst, K.; Domingo, N.; Cavallini, M.; Biscarini, F.; Tejada, J.; Rovira, C.; Veciana, J. *Nat. Mater.* **2003**, *2*, 190–195.
(26) Ohkoshi, S. I.; Arai, K. I.; Sato, Y.; Hashimoto, K. *Nat. Mater.* **2004**, *3*, 857–861.
(27) Ohba, M.; Yoneda, K.; Agusti, G.; Munoz, M. C.; Gaspar, A. B.; Real, J. A.; Yamasaki, M.; Ando, H.; Nakao, Y.; Sakaki, S.; Kitagawa, S. *Angew. Chem., Int. Ed.* **2009**, *48*, 4767–4771.
(28) Southon, P. D.; Liu, L.; Fellows, E. A.; Price, D. J.; Halder, G. J.; Chapman, K. W.; Moubaraki, B.; Murray, K. S.; Letard, J. F.; Kepert, C. J. *J. Am. Chem. Soc.* **2009**, *131*, 10998–11009.

 Published on Web 12/02/2010

Table 1. Crystallographic Data for [M(TCNQ)bpy]·*x*MeOH (M = Zn, Mn, Co, Cd)

	Zn	Mn	Co	Cd
formula	$C_{28}H_{30}N_6O_6Zn$	$C_{57}H_{76}Mn_2N_{12}O_{13}$	C_{30} Co N_6 O_8	$C_{30}H_{10}CdN_6O_8$
fw	611.96	1247.18	631.30	694.85
cryst syst	tetragonal	tetragonal	tetragonal	tetragonal
space group	*P*4/*ncc* (#130)	*P*4/*ncc* (#130)	*P*4/*ncc* (#130)	*P*4/*ncc* (#130)
a, Å	17.355(1)	17.2551(4)	17.302(8)	17.571(14)
c, Å	22.740(2)	23.1856(7)	22.789(11)	23.404(18)
V, Å^3	6848.7(10)	6903.2(3)	6822(6)	7226(10)
Z	8	4	8	8
temp, K	213	130	223	223
R1 [$I > 2\sigma(I)$] [a]	0.074	0.0517	0.0869	0.0504
wR2 [$I > 2\sigma(I)$] [a]	0.081	0.1336	0.1209	0.0560
GOF	1.087	0.906	1.059	1.052
reference	ref 29	ref 45	this work	this work

[a] $R1 = \sum||F_o| - |F_c||/\sum|F_o|$; $wR2 = [\sum w(F_o^2 - F_c^2)^2/\sum w(F_o^2)^2]^{1/2}$.

metal ions contribute to the diversity of PCPs in a different way. However, there is only a finite variation of metal ions, which is much less than that of organic ligands, providing the structural multiplicity of the coordination geometry, including coordination number and distortion of bond angles. Moreover, they provide high diversity, such as flexibility based on the dynamics of coordination bonds and electronic/magnetic properties based on their charge states. Usually, metal ions act as the nodes of the framework and have less opportunity to interact directly with guest molecules. However, it is conceivable that metal ions could strongly impact the host−guest interaction if they interact electronically with the organic ligands.

We have previously reported several PCPs with 7,7,8,8-tetracyano-*p*-quinodimethane (TCNQ) as an organic ligand,[29,30] focusing on the electrical and structural properties of this organic molecule. TCNQ is a well-known multiredox active organic molecule that can act as a good acceptor and a weak or a strong donor when its valence is 0, −1, or −2, respectively.[31−34] In addition, TCNQ is suitable for forming high-dimensional coordination networks because of the coordination and structural diversities based on its multidentate nature and dimerization reaction.[35−42] The TCNQ in the frameworks acts as a good interaction site for guest adsorption and recognition, resulting in it showing unique sorption properties such as selective organic and gas sorption,[30] as well as guest-responsive color changes based on the charge-transfer (CT) interaction.[29] In contrast to the organic ligands, the metal ions are not considered to be the important component for the unique porous properties in these PCP systems. However, an exploration of the metal-dependent porous properties of PCPs is also an intriguing topic and has great potential for exploiting a new field of PCPs. In this paper, five PCPs [M(TCNQ)bpy] (M = Fe(II), Zn(II), Mn(II), Co(II), Cd(II), bpy = 4,4′-bipyridyl) consisting of the same components except for the metal cations and forming identical structures were prepared to compare the metal-dependent porous and electronic properties.

Experimental Section

Materials. All chemicals and solvents used in the syntheses were reagent grade. LiTCNQ was prepared by the literature method;[43] the solution of TCNQ (1.02 g, 5 mmol) and lithium iodide (1.00 g, 7.5 mmol) in acetonitrile (50 mL) was mixed in reflux condition for 12 h under an N_2 atmosphere. After cooling, the purple powder was separated by filtration and washed with acetonitrile until the washings were bright green.

Synthesis of [M(TCNQ)bpy] (M = Fe, Zn, Mn, Co, Cd). All procedures were carried out under an N_2 atmosphere using the Schlenk technique. Single crystals suitable for X-ray analysis were prepared by careful diffusion of a solution of LiTCNQ (0.1 mmol, 21 mg) and bpy (0.1 mmol, 16 mg) in methanol (20 mL) into a solution containing metal(II) nitrate hydrate (Mn, Co, Zn, Cd) or ammonium iron(II) sulfate hydrate (0.1 mmol), and a small amount of ascorbic acid in methanol/water mixture (10 mL/10 mL) in a straight glass tube. Crystals began to form in a few days. The bulk product was obtained by slow addition of a solution of LiTCNQ (1 mmol, 211 mg) and bpy (1 mmol, 156 mg) in methanol (20 mL) to a solution of metal(II) nitrate hydrate (Mn, Co, Zn, Cd) or ammonium iron(II) sulfate hydrate (1 mmol), and ascorbic acid (1 mmol, 176 mg) in methanol/water mixture (10 mL/10 mL). Powder samples were collected by filtration and washed with methanol, then immediately soaked in an aromatic solvent (such as nitrobenzene) to exchange the guest molecules without drying in the process. After further filtration, the powder samples were lightly dried. (yield ca. 75%)

Physical Measurements. Infrared spectra were measured using a KBr disk with a Perkin-Elmer Spectrum 2000 FT-IR system. X-ray powder diffraction (XRPD) data were collected on a Rigaku RINT-2200HF (Ultima) diffractometer with Cu−Kα radiation (λ = 1.54073 Å). UV−vis spectra were recorded on a HITACHI U-3500/U-4000 spectrometer.

Crystal Structure Determination. X-ray diffraction data of all compounds (Tables 1 and 2) were collected on a Rigaku Mercury

(29) Shimomura, S.; Matsuda, R.; Tsujino, T.; Kawamura, T.; Kitagawa, S. *J. Am. Chem. Soc.* **2006**, *128*, 16416–16417.
(30) Shimomura, S.; Horike, S.; Matsuda, R.; Kitagawa, S. *J. Am. Chem. Soc.* **2007**, *129*, 10990–10991.
(31) Acker, D. S.; Harder, R. J.; Hertler, W. R.; Mahler, W.; Melby, L. R.; Benson, R. E.; Mochel, W. E. *J. Am. Chem. Soc.* **1960**, *82*, 6408–6409.
(32) Clarkson, S. G.; Lane, B. C.; Basolo, F. *Inorg. Chem.* **1972**, *11* 662–664.
(33) Kistenmacher, T. J.; Emge, T. J.; Bloch, A. N.; Cowan, D. O. *Acta Crystallogr., Sect. B: Struct. Sci.* **1982**, *38*, 1193–1199.
(34) Miller, J. S.; Zhang, J. H.; Reiff, W. M.; Dixon, D. A.; Preston, L. D.; Reis, A. H.; Gebert, E.; Extine, M.; Troup, J.; Epstein, A. J.; Ward, M. D. *J. Phys. Chem.* **1987**, *91*, 4344–4360.
(35) Shields, L. *J. Chem. Soc., Faraday Trans. 2* **1985**, *81*, 1–9.
(36) Kaim, W.; Moscherosch, M. *Coord. Chem. Rev.* **1994**, *129*, 157–193.
(37) Ballester, L.; Gutierrez, A.; Perpinan, M. F.; Azcondo, M. T. *Coord. Chem. Rev.* **1999**, *192*, 447–470.
(38) Zhao, H.; Heintz, R. A.; Ouyang, X.; Dunbar, K. R.; Campana, C. F.; Rogers, R. D. *Chem. Mater.* **1999**, *11*, 736–746.
(39) Heintz, R. A.; Zhao, H. H.; Xiang, O. Y.; Grandinetti, G.; Cowen, J.; Dunbar, K. R. *Inorg. Chem.* **1999**, *38*, 144–156.
(40) Miyasaka, H.; Campos-Fernandez, C. S.; Clerac, R.; Dunbar, K. R. *Angew. Chem., Int. Ed.* **2000**, *39*, 3831–3835.
(41) Abrahams, B. F.; Hudson, T. A.; Robson, R. *Cryst. Growth Des.* **2008**, *8*, 1123–1125.
(42) Miyasaka, H.; Motokawa, N.; Matsunaga, S.; Yamashita, M.; Sugimoto, K.; Mori, T.; Toyota, N.; Dunbar, K. R. *J. Am. Chem. Soc.* **2010**, *132*, 1532–1544.
(43) Melby, L. R.; Mahler, W.; Mochel, W. E.; Harder, R. J.; Hertler, W. R.; Benson, R. E. *J. Am. Chem. Soc.* **1962**, *84*, 3374–3387.

Table 2. Crystallographic Data for [Fe(TCNQ)bpy]·Guest at 133 K (Fe_133K), 243 K (Fe_243K), and with Anisole (Fe⊃ani) and Nitrobenzene (Fe⊃nb)

	Fe_133K	Fe_243K	Fe⊃ani	Fe⊃nb
formula	$C_{29}H_{33}FeN_6O_7$	$C_{30}H_{12}FeN_6O_8$	$C_{22}H_{12}FeN_6$	$C_{22}H_{12}FeN_6$
fw	633.46	640.31	416.22	416.22
cryst syst	tetragonal	tetragonal	tetragonal	tetragonal
space group	$P\bar{4}2_1c$ (#114)	$I4/mcm$ (#140)	$I4/mcm$ (#140)	$P4/ncc$ (#130)
a, Å	17.2926(4)	12.413(20)	12.377(13)	17.4656(7)
c, Å	22.8962(8)	23.03(4)	22.90(2)	23.0745(11)
V, Å^3	6846.7(3)	3549(10)	3508(6)	7038.8(5)
Z	8	4	4	8
temp, K	133	243	213	293
R1 [$I > 2\sigma(I)$] [a]	0.0749	0.0873	0.0853	0.1776
wR2 [$I > 2\sigma(I)$] [a]	0.1039	0.1036	0.0806	0.2072
GOF	1.139	1.041	0.841	1.069
reference	this work	this work	this work	this work

[a] $R1 = \sum||F_o| - |F_c||/\sum|F_o|$; $wR2 = [\sum w(F_o^2 - F_c^2)^2/\sum w(F_o^2)^2]^{1/2}$.

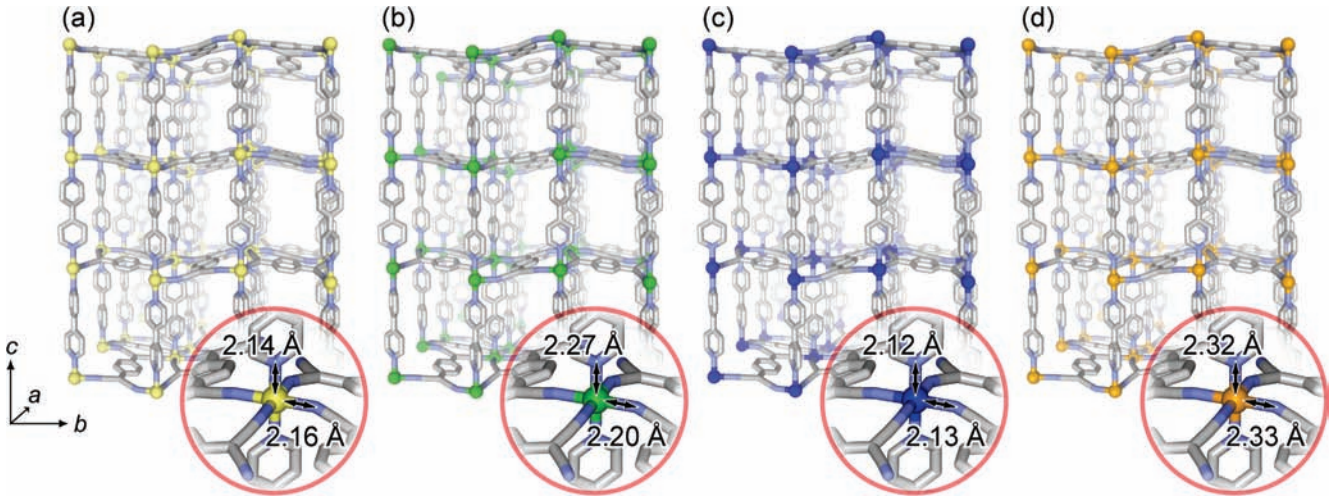

Figure 1. Crystal structures of [M(TCNQ)bpy]·xMeOH (M = (a) Zn, (b) Mn, (c) Co, (d) Cd) showing the pillared layer structures and the averaged coordination bond lengths. In the Mn complex, the values of bond lengths extracted from the structure measured at 223 K to remove the temperature effect. One of the doubly disordered bpy, the hydrogen atoms, and guest molecules, methanol, are omitted for clarity.

CCD system with graphite monochromated Mo K radiation and a Rigaku/MSC Saturn CCD diffractometer with confocal monochromated Mo Kα radiation (λ = 0.71070 Å). Single crystals were mounted in a quartz tube filled with solvent vapors to avoid drying, and kept at measurement temperature under flowing N_2 during collection of the diffraction data. The crystal structures were solved by a direct method (SIR2002 and SHELX97) and refined by full-matrix least-squares refinement using the CRYSTALS computer program. The positions of nonhydrogen atoms were refined with anisotropic displacement factors, except for the guest molecules. The hydrogen atoms were positioned geometrically and refined using a riding model. CCDC 784861−784866 contain the supporting crystallographic data for this paper. These data can be obtained free of charge from The Cambridge Crystallographic Data Centre via www.ccdc.cam.ac.uk/data_request/cif.

Results and Discussion

The crystals of [M(TCNQ)bpy] were obtained by the complexation reaction of the divalent metal cations, TCNQ dianion, and bpy in solution at room temperature. Two synthesis methods have been previously reported: a disproportionation reaction of TCNQ radical anions[29,44] and a deprotonation reaction of $TCNQH_2$ to generate TCNQ dianion.[45] We optimized the reaction conditions of the former method and found that the disproportionation reaction of TCNQ radical anions to produce TCNQ dianion was facilitated by the presence of ascorbic acid in the solution. Ascorbic acid, which is a good reducing agent, promotes the reduction reaction even on radical anionic molecules, forming dianion species. In the absence of ascorbic acid, some side reactions easily occurred, and it was very difficult to obtain the pure [M(TCNQ)bpy] compounds by this method. The latter method was recently reported and adopted by Robson and co-workers.[45] The as-synthesized compounds immediately show an irreversible transformation on exposure to air because of the immediate removal of guest molecules of methanol, resulting in a nonporous compound. However, these compounds undergo guest exchange from the methanol to aromatic molecules, such as nitrobenzene, when they are immersed in the neat solvent. The aromatic guest molecules, which are slow to be released from the framework, make the compounds air stable because of the strong interaction between the guest molecules and the framework. Single-crystal X-ray analysis of [M(TCNQ)bpy] revealed tetragonal structures in which the metal ions were connected4 by TCNQ dianions to form two-dimensional sheet motifs parallel to the *ab*-plane, and they were linked by bpy ligands along the *c*-axis to give three-dimensional pillared layer-type networks (Figures 1, 2). The

(44) Grossel, M. C.; Duke, A. J.; Hibbert, D. B.; Lewis, I. K.; Seddon, E. A.; Horton, P. N.; Weston, S. C. *Chem. Mater.* **2000**, *12*, 2319–2323.
(45) Abrahams, B. F.; Elliott, R. W.; Hudson, T. A.; Robson, R. *Cryst. Growth Des.* **2010**, *10*, 2860–2862.

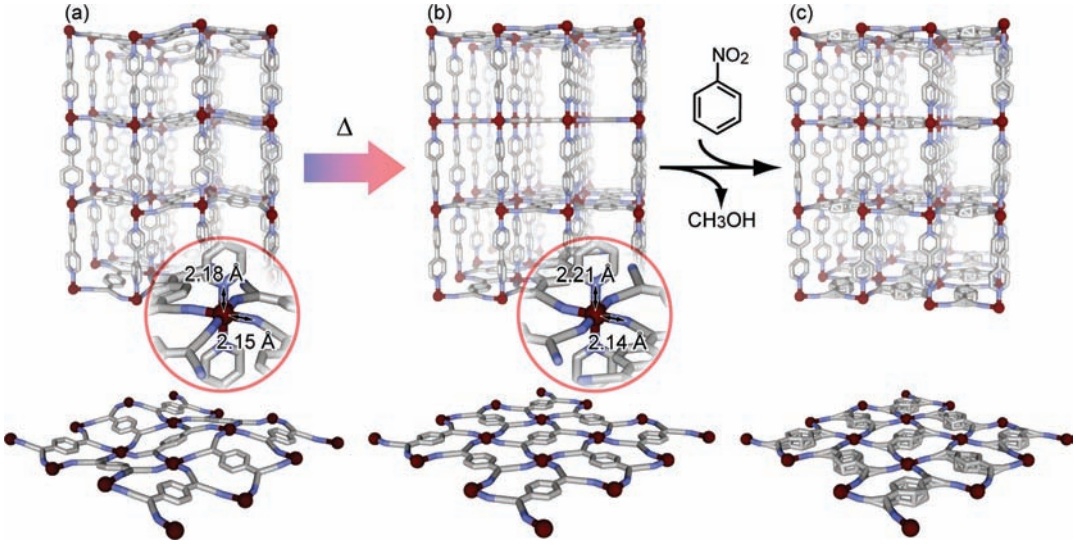

Figure 2. Crystal structures of [Fe(TCNQ)bpy]·*x*MeOH at (a) 133 K and (b) 243 K, and (c) obtained after guest exchange with nitrobenzene. Bottom parts show the forms of the two-dimensional layers [Fe(TCNQ)] in each structure. One of the doubly disordered bpy, the hydrogen atoms, and guest molecules are omitted for clarity.

Table 3. Bond Lengths (Å) of TCNQ Moiety in [M(TCNQ)bpy]·*x*MeOH and Related Compounds

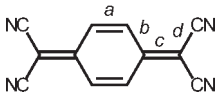

	a	*b*	*c*	*d*	$I = c/(b + d)$
$TCNQ^{-}$ [a]	1.373(4)	1.423(4)	1.420(4)	1.416(4)	0.500
$TCNQ^{2-}$ [b]	1.371(9)	1.39(1)	1.481(9)	1.38(1)	0.535
	1.380(9)	1.397(9)	1.491(9)	1.39(1)	0.535
Fe_133K	1.383(3)	1.397(3)	1.480(3)	1.394(3)	0.530
Fe_243K	1.362(4)	1.380(4)	1.462(4)	1.403(4)	0.525
Fe⊃ani	1.403(5)	1.389(4)	1.468(3)	1.392(4)	0.528
Zn [c]	1.377(6)	1.398(6)	1.477(5)	1.392(5)	0.529
Mn [d]	1.376(4)	1.407(4)	1.461(4)	1.398(4)	0.521
Co	1.383(9)	1.386(8)	1.475(8)	1.399(8)	0.530
Cd	1.379(6)	1.395(6)	1.469(6)	1.391(6)	0.527

[a] Reference 33. [b] Reference 46. [c] Reference 29. [d] Reference 45.

structure of the Mn complex is similar to the structure that has already been reported.[45] The as-synthesized two-dimensional motifs of metal ions and TCNQ dianions mainly show corrugated layer structures at the measurement temperature except for the Fe complex. At low temperature (133 K), the Fe complex also shows a similar corrugated layer structure (Figure 2a). However, the layer transforms to a flattened structure and the symmetry changes from primitive lattice (P) to body-centered lattice (I) when the compound is heated to 243 K (Figure 2b). In this transformation, a slight tetragonal distortion, with expansion in the Fe−N(bpy) axial bonds (from 2.18 Å to 2.21 Å, on average) and almost no change in the Fe−N(TCNQ) equatorial bonds (from 2.15 Å to 2.14 Å), and a reduction in the deviation of the π-surface of TCNQ from the *ab*-plane were observed. In addition, the structure of TCNQ in the framework changes with this transformation. In the context of electronic issues, the most important structural features in TCNQ complexes are the bond lengths within the

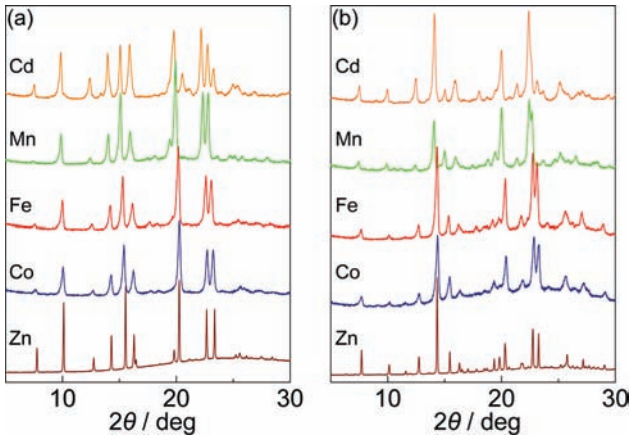

Figure 3. XRPD patterns of [M(TCNQ)bpy] (M = Fe, Zn, Mn, Co, Cd) with (a) anisole and (b) nitrobenzene as the guest molecules.

TCNQ ligand. The C−C distances within the TCNQ ring are a good indicator of the oxidation state.[33,40,46] The small decrease in the value of the relationship of bond lengths of TCNQ ($I = c/(b + d)$) implies that the ligand loses a partial negative charge in this transformation (Table 3). This would be strongly involved with the change of the Fe−TCNQ bond.

The three-dimensional structures of [M(TCNQ)bpy] possess two-dimensional grid-like pores filled with the methanol molecules, as previously described. The accessible spaces are surrounded by TCNQ dianions, which have a strong electron-donating ability to make CT interactions with electron-accepting molecules. These frameworks show CT-induced color changes depending on the electron-accepting ability of the guest molecules.[29] We used two aromatic molecules, anisole and nitrobenzene, possessing different electron-accepting ability, to evaluate the CT character of these complexes. In the case of the Fe complex, despite a lack of color change with anisole, the red crystal quickly turns dark brown by guest exchange with nitrobenzene. We tried to elucidate the details of the difference by single-crystal X-ray diffraction analysis. The Fe complex with anisole (Fe⊃ani) shows a simple pillared layer structure with a planar two-dimensional layer,

(46) Oshio, H.; Ino, E.; Ito, T.; Maeda, Y. *Bull. Chem. Soc. Jpn.* **1995**, *68*, 889–897.

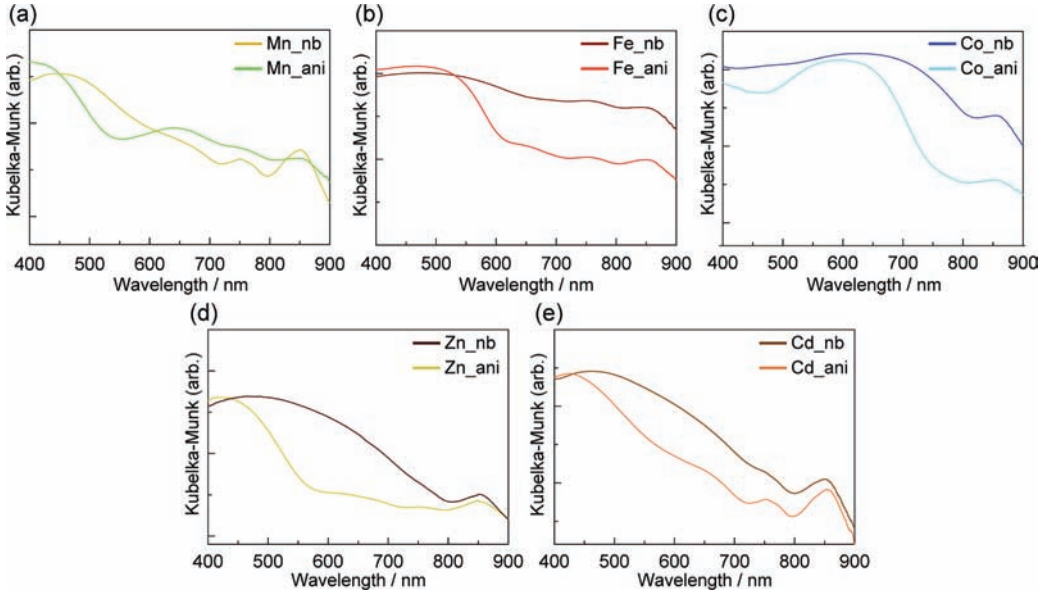

Figure 4. Diffuse reflectance UV−vis spectra of [M(TCNQ)bpy] (M = (a) Mn, (b) Fe, (c) Co, (d) Zn, (e) Cd) with anisole (M_ani) and nitrobenznen (M_nb).

which was observed in the as-synthesized form at ambient temperature. TCNQ moieties in the framework do not have a disordered structure, and the value of *I*, which is a good indicator of the oxidation state, is almost the same as that of the as-synthesized form. Only low electron density was observed in the pore, and the positions of the guest molecules could not be determined, probably because of their disordered distributions. In contrast, in the Fe complex with nitrobenzene (Fe⊃nb), the TCNQ moieties in the framework have a chaotic structure; the TCNQ ring was strongly disordered in the vertical direction to the slightly corrugated two-dimensional layer (Figure 2c). Although the arrangement of the guest molecules in the pore also was not determined, some electron density close to the π-surface of TCNQ can be observed. These results imply that there are some differences in electronic state between the TCNQ moieties of Fe⊃ani and Fe⊃nb, the differences being induced by the host−guest CT interactions, given the spectroscopic results described below. The results of TGA measurement of Fe⊃nb and Fe⊃ani showed the framework contained 2.3 nitrobenzene molecules and 2.2 anisole molecules per formula, respectively. In cases of the other metal cations, the amounts of guest molecules are below: [Zn(TCNQ)bpy]⊃ 3.3 ani or 3.2 nb, [Mn(TCNQ)-bpy]⊃ 2.0 ani or 2.6 nb, [Co(TCNQ)bpy]⊃ 2.7 ani or 1.8 nb, [Cd(TCNQ)bpy]⊃ 2.6 ani or 2.9 nb. We also measured the XRPD patterns of all metal complexes after guest exchange (Figure 3). There were clear differences in the relative intensities between the patterns of the anisole forms and the nitrobenzene forms. However, we could not observe a clear metal dependence in the patterns with each guest molecule.

Figure 4 shows the solid state UV−vis spectra of [M(TCNQ)bpy] with anisole and nitrobenzene. In previous work on the Zn complex, a shift in the absorption band associated with the electron-accepting characteristics of the guest molecule was observed.[29] All complexes also show guest-responsive absorption bands; a red shift of the adsorption bands of M⊃nb around 400−700 nm from the bands of M⊃ani (M⊃ani to M⊃nb, Fe: 472 to 478 nm, Zn: 418 to 480 nm, Mn: < 400 to 447 nm, Co: 595 to 626 nm, Cd: 424 to 462 nm). Furthermore, the absorption region of the nitrobenzene compounds tend to be broader to low energy region than those of the anisole compounds, especially in the case of the Fe complex. This is ascribed to the CT interaction between the host frameworks and the aromatic molecules. The peak positions and the responsiveness to guest molecules vary according to the metal ions. If metal ions have no effect on the electronic state of TCNQ in the frameworks, no differences would be observed in their absorption bands. It seems that the metal ions electronically interact with TCNQ and, although there are some differences of degree, affect the electron configuration of TCNQ. Infrared spectroscopy in the ν(C≡N) region is useful for assigning charge as well as predicting stacking modes in TCNQ complexes. However, for identification of oxidation state of TCNQ, analysis of the IR data for metal-bound TCNQ ligands is complicated by the fact that ν(C≡N) stretches can shift to higher energies if the TCNQ acts primarily as a σ-donor or to lower energies if there is significant metal-to-TCNQ π-back bonding.[36−38] Therefore, we compared the more informative infrared active modes, δ(C−H) bend, to understand the change in electronic states of the TCNQ moieties. All complexes exhibit a δ(C−H) mode at almost the same position around 825 cm^{-1} in accord with the presence of reduced TCNQ (Figure 5b).[38,47] In contrast to the δ(C−H) modes, there are some differences depending on the metal ions in the ν(C≡N) modes (Figure 5a). The frequency of the ν(C≡N) mode decreases in the following order: Zn, Co, Mn, Fe. In the case of the Cd complex, peak splitting of the ν(C≡N) bands was observed, which comes from the existence of several ν(C≡N) modes in the complex. However, we have no structural information or additional spectroscopic data; the completely occupied d-orbitals and/or the size of the metal ion may lead to this peak splitting, considering the subtle but similar tendency in the Zn complex. The M−TCNQ coordination bonding characteristics such as σ-bonding and π-back bonding depend on the metal ions. This difference is the linchpin of the various properties of the whole framework in these systems.

(47) Khatkale, M. S.; Devlin, J. P. *J. Chem. Phys.* **1979**, *70*, 1851–1859.

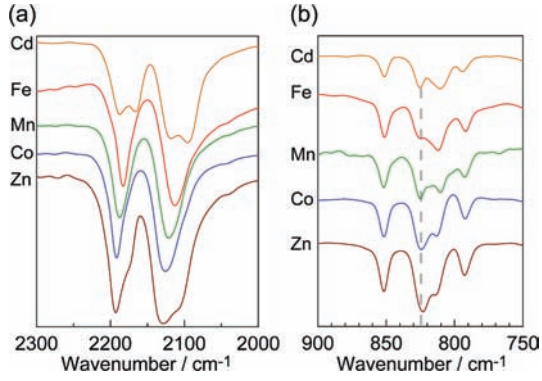

Figure 5. Infrared spectra around (a) the ν(C≡N) and (b) δ(C−H) region of [M(TCNQ)bpy] (M = Fe, Zn, Mn, Co, Cd) with nitrobenzene.

As a preliminary experiment, we checked the electrical resistivity of these compounds at room temperature. The compounds used for this measurement were pressed into pellets at about 13 MPa. They showed high resistivity in the region between semiconductor and insulator. In case with nitrobenzene as the guest, the Fe complex showed the lowest resistivity (5.9×10^7 Ω cm) and the Zn complex showed the highest resistivity ($> 10^{11}$ Ω cm). When the guest was exchanged from nitrobenzene to anisole, the resistivity increased by about 100-fold. These results imply that the TCNQ units, metal ions, and guest molecules have an electronic relationship with each other.

Conclusion

This paper has described the synthesis and characterization of a series of TCNQ-dianion-based PCPs [M(TCNQ)bpy] (M = Fe, Zn, Mn, Co, Cd). They form three-dimensional pillared layer structures composed of M−TCNQ two-dimensional layers and bpy pillars regardless of the metal ions. They show metal-dependent guest-responsive color changes and electronic properties. This indicates that the metal ions acting as a node in the frameworks electronically interact with TCNQ moieties and affect the molecular orbitals of TCNQ. These systems with an electronic relationship between metal ions, organic ligands, and guest molecules are still not common, but should be important in creating new porous properties in the field of PCPs. They have the potential to provide a new platform to synthesize organic−inorganic hybrid functional materials.

Acknowledgment. This work was supported by an ERATO JST Project "Kitagawa Integrated Pores Project".

Supporting Information Available: X-ray crystallographic data for the structure determinations of [M(TCNQ)bpy] (M = Fe, Co, Cd) in CIF format. This material is available free of charge via the Internet at http://pubs.acs.org.